PCCP

Theoretical evidence of water serving as a promoter for lithium superoxide disproportionation in Li-O_2 batteries

Journal:	*Physical Chemistry Chemical Physics*
Manuscript ID	CP-ART-11-2020-005924.R3
Article Type:	Paper
Date Submitted by the Author:	28-Feb-2021
Complete List of Authors:	Shan, Nannan; Argonne National Laboratory, Materials Science Division Redfern, Paul; Argonne National Laboratory, Materials Science Division Ngo, Anh; Argonne National Laboratory, Materials Science Division; University of Illinois at Chicago, Department of Chemical Engineering Zapol, Peter; Argonne National Laboratory, Materials Science Division Markovic, Nenad; Argonne National Laboratory, Materials Science Division Curtiss, Larry; Argonne National Laboratory, Materials Science Division

Theoretical evidence of water serving as a promoter for lithium superoxide disproportionation in Li-O_2 batteries

Nannan Shan,[1] Paul C. Redfern,[1] Anh T. Ngo,[1,2] Peter Zapol,[1] Nenad Markovic,[1] Larry A. Curtiss[1]*

[1] Materials Science Division, Argonne National Laboratory, Lemont, IL, 60439, USA

[2] Department of Chemical Engineering, University of Illinois at Chicago, Chicago, IL, 60607, USA

*Larry A. Curtiss: curtiss@anl.gov

Abstract

Experimental evidence has demonstrated that the presence of water in non-aqueous electrolytes significantly affects Li-O_2 electrochemistry. Understanding the reaction mechanism for Li_2O_2 formation in the presence of water impurities is important to understand Li-O_2 battery performance. A recent experiment has found that very small amounts of water (as low as 40 ppm) can significantly affect the product formation in Li-O_2 batteries as opposed to essentially no water (1 ppm). Although experimental as well as theoretical work has proposed mechanisms of Li_2O_2 formation in the presence of much larger amounts of water, none of the mechanisms provide an explanation for the observations for very small amounts of water. In this work, density functional theory (DFT) was utilized to obtain a mechanistic understanding of the Li-O_2 discharge chemistry in a dimethoxyethane (DME) electrolyte containing an isolated water and no water. The reaction pathways for Li_2O_2 formation from LiO_2 on a model system were carefully evaluated with different level of theories, i.e. PBE (PW), B3LYP/6-31G(2df,p), B3LYP/6-311++G(2df,p) and G4MP2. The results indicate that the LiO_2 disproportionation reaction to Li_2O_2 can be promoted by the water in DME electrolyte, which explains why there is a significant difference compared to when no water is present in the experimentally observed discharge product distributions. Ab initio molecular dynamics calculations were also used to investigate the disproportionation of LiO_2 dimer in explicit DME. This work adds to the fundamental understanding of the discharge chemistry of a Li-O_2 battery.

1. Introduction

The lithium-oxygen (Li-O_2) battery is being extensively studied as a technology to address future energy storage challenges due to its potential for a high theoretical energy density.[1-4] The high energy density is due to the formation of lithium peroxide or other lithium oxides as the discharge product, which can store large amounts of energy in chemical bonds.[5-8] In a Li-O_2 battery, an oxygen cathode is used to accumulate the solid products generated from the reaction of Li cations with O_2 during discharge. The cathode may contain a catalyst in some forms to promote the discharge product formation as well as decomposition during charge. Studies have found that various factors can dictate the electrochemical reactions including the nature of the catalyst or the catalyst support, the type and amount of organic electrolyte used, electrolyte impurities and the current rate.[9-13] The development of batteries based on the formation and decomposition of lithium-oxygen bond requires fundamental understanding of Li-O_2 electrochemistry, whereby a product such as lithium peroxide (Li_2O_2) is formed during discharge and decomposed during charge.

One interesting aspect of the Li-O_2 discharge chemistry is that addition of different amounts of water to the electrolyte can have a significant effect on Li_2O_2 morphology and discharge capacity in a Li-O_2 battery.[14-18] Luntz et al[15] found that adding 500-4000 ppm H_2O to the dimethoxyethane (DME) electrolyte could promote Li_2O_2 toroid formation on the cathode, while in the anhydrous (<30 ppm H_2O) electrolyte, a thin Li_2O_2 film was observed. Increased discharge capacity was also observed in the electrolyte with 500-4000 ppm water. Work from Shao-Horn's group[17] indicated that the decreased surface Li_2O_2 nucleation rate in DME-based electrolyte containing 5000 ppm H_2O was the reason for the increased capacity. Gasteiger and coworkers[16] suggested that different water concentrations (200 and 1000 ppm) in diglyme electrolyte can result in various enhanced amounts of discharge capacity. In addition to these studies, a very careful systematic study by Markovic et al[18] compared 1 ppm and 40 ppm water in a DME electrolyte and revealed an interesting dependence of the resulting discharge product on the water concentration. The key conclusion based on Raman spectroscopy[18] is that, the formation of Li_2O_2 (identified by a peak at 785 cm^{-1}, which corresponds to Li_2O_2 according to Ref 19) is promoted in the electrolyte with 40 ppm of water while LiO_2 is the main product in the 'dry' electrolyte (1 ppm). It is also surprising

that the 40 ppm of water is not consumed in promoting Li_2O_2 formation, even after a prolonged discharge reaction time.

Both experimental and theoretical efforts have been devoted to understanding the reaction mechanisms for Li_2O_2 formation involving water presence in different conventional electrolytes. It is believed that water can promote the solution-based mechanism for Li_2O_2 formation by different reaction pathways.[15, 20, 21] Luntz et al[15] proposed that the LiO_2 solubility was improved by a certain amount of water (500-4000 ppm), which results in the $O_2^-(sol)$ anion being available as a redox shuttle to promote the solution-mediated growth of Li_2O_2. With 10 M water in dimethyl sulfoxide (DMSO) electrolyte, the activity of O_2 to O_2^- was enhanced resulting in a Li_2O_2 solution-driven pathway.[20] Zhou and co-workers[21] proposed that OOH^- instead of O_2^- was the active species and peroxide source for Li_2O_2 formation. Another explanation is that water serves as the proton source to react with Li_2O_2 and could benefit LiOH/LiOOH cycling during discharge and charge reactions in the electrolytes in the presence of large amount of water.[22-27]

However all the mechanisms mentioned above do not explain the reported finding[18] that very small amounts of water promotes Li_2O_2 formation. Therefore, the focus of this work is to develop an explanation for how very small amounts of water can affect the discharge chemistry such as found in the study of Markovic et al.[18] The effect of very small amounts of water is of interest because many electrolytes have water present as a minor impurity and its effect on the Li-O_2 electrochemistry is generally neglected or unknown. In this work, a model with one H_2O molecule was used to represent an electrolyte with very small amount water (40 ppm), i.e. 'wet' electrolyte, as named in the experimental study of Markovic et al[18], while a model without a H_2O molecule represents the 'dry' electrolyte. It is also noted that for a system with 40 ppm water there would be one H_2O molecule per 5000 solvent molecules so that our model for the 'wet' electrolyte should be reasonable.

Various possible reactions, both electrochemical and chemical, can be involved in the discharge process of a Li-O_2 battery. The net discharge reaction typically produces lithium peroxide (Li_2O_2) via the oxidation of metallic lithium as in Reaction (1).

$$2Li + O_2 \rightarrow Li_2O_2 \quad (1)$$

One of the possible pathways to Li_2O_2 in a Li-O_2 battery involves disproportionation of lithium superoxide (LiO_2), the result of a one-electron reaction, as introduced by Abraham et al[28] and shown in Reactions (2,3).

$$Li^+ + e^- + O_2 \rightarrow LiO_2 \quad (2)$$

$$2LiO_2 \rightarrow Li_2O_2 + O_2 \quad (3)$$

Alternatively, a two-electron reaction can result in the direct formation of Li_2O_2.

$$2Li^+ + 2e^- + O_2 \rightarrow Li_2O_2 \quad (4)$$

The LiO_2 dimer disproportionation reaction without water present has been studied theoretically.[29, 30] In this paper we report detailed density functional (DFT) and ab initio molecular dynamics (AIMD) calculations on how the presence of an isolated H_2O molecule might act to promote disproportionation of LiO_2 to Li_2O_2 (Reaction (3)). The two-electron reaction mechanism in Reaction (4) on an Au surface is also investigated to determine whether the presence of the surface has an effect.

2. Computational methods

The LiO_2 disproportionation reaction was investigated with DFT calculations using the B3LYP functional[31, 32] and PBE(PW) functional[33] with spin-polarization and a plane wave basis (PW). The B3LYP calculations were conducted with the Gaussian 09 program.[34] The PBE(PW) calculations were carried out with the Vienna Ab Initio Simulation Package (VASP) using the periodic boundary condition.[35] The detailed parameters for PBE calculations can be found in Electronic Supplementary Information (ESI). The B3LYP geometry optimizations and transition state searches were performed using the 6-31G(2df,p) basis set. Then the single point energies were calculated with the 6-311++G(2df,p) basis set. In addition, the G4MP2 method,[36] a composite wave function based method, is also employed, which should be the most accurate method as it is based on CCSD(T) with an estimate for effects of larger basis sets. The G4MP2 composite method uses optimized geometries from the B3LYP/6-31G(2df,p) theory to obtain the reaction energies

and energy barriers.[37, 38] The PCM continuum solvation method[39, 40] was used for implicit solvation calculations of solvation energies with a dielectric (7.2) corresponding to dimethoxyethane (DME). The B3LYP/6-31G(2df,p) harmonic vibrational frequencies scaled by 0.985 were used for the zero-point energies approximation.[41, 42]

The free energies (G) of the species in gas phase obtained based on B3LYP/6-31G(2df,p), B3LYP/6-311++G(2df,p) and G4MP2 theories were calculated according to Equation (5),

$$G = H - TS, \quad (5)$$

where $H = E_o + ZPE + E_{tr} + E_{rot} + E_{vib} + pV$. Here E_o is the electronic energy, ZPE is the zero-point energy, E_{tr} is the translational energy, E_{rot} is the rotational energy, E_{vib} is the temperature correction to the vibrational energy, and pV is RT. The free energy with solvation effects included from an implicit solvation model is referred to as G_{sol}. The method used for free energy estimation for the PBE(PW) calculations and solvation effects can be found in ESI.

The AIMD calculations with VASP were carried out to investigate the disproportionation reaction discussed above with explicit DME electrolyte molecules. The generalized gradient approximation Perdew−Burke−Ernzerhof (GGA-PBE) functional[33] was employed to obtain the exchange-correlation energies, while projector-augmented wave (PAW) method[43] was adopted to describe core-valence interactions. A kinetic energy cutoff of 500 eV was applied for the plane wave orbitals. The Brillouin zone in the reciprocal space was sampled using the Γ-point only. The electronic self-consistent calculation was converged when the energy difference fell below 10^{-5} eV. All the calculations were spin-polarized. The canonical (NVT) ensemble was used with a constant temperature (i.e. 300K) controlled with a Nosé-Hoover thermostat.[44] The AIMD simulations were run for 2 picosecond (ps) with the equations of motion integrated with a time step of 1 femtoseconds (fs). A $18 \times 18.1 \times 18.3$ Å^3 simulation box filled with 34 DME molecules was utilized for the AIMD calculations.

3. Results and discussion

The reaction free energies, ΔG_{sol}, for the LiO_2 dimer disproportionation reaction with a water molecule (denoted as 'wet' environment) and without a water molecule (denoted as 'dry' environment) based on the G4MP2 level of theory are plotted by blue and black lines, respectively, in Figure 1. The results are relative to the energies of either a complex of a H_2O-$(LiO_2)_2$ complex or a LiO_2 dimer for these two environments, respectively. The reaction network involves the initial reactants (H_2O-$(LiO_2)_2$ complex or LiO_2 dimer), the transition states (H_2O-$(LiO_2)_2$TS or $(LiO_2)_2$TS), the disproportionation intermediate structures (H_2O-Li_2O_2-O_2 complex or Li_2O_2-O_2 complex), and the final products (H_2O-Li_2O_2 plus O_2 or Li_2O_2 plus O_2). The geometries of relevant species are shown in the top and bottom panels of Figure 1.

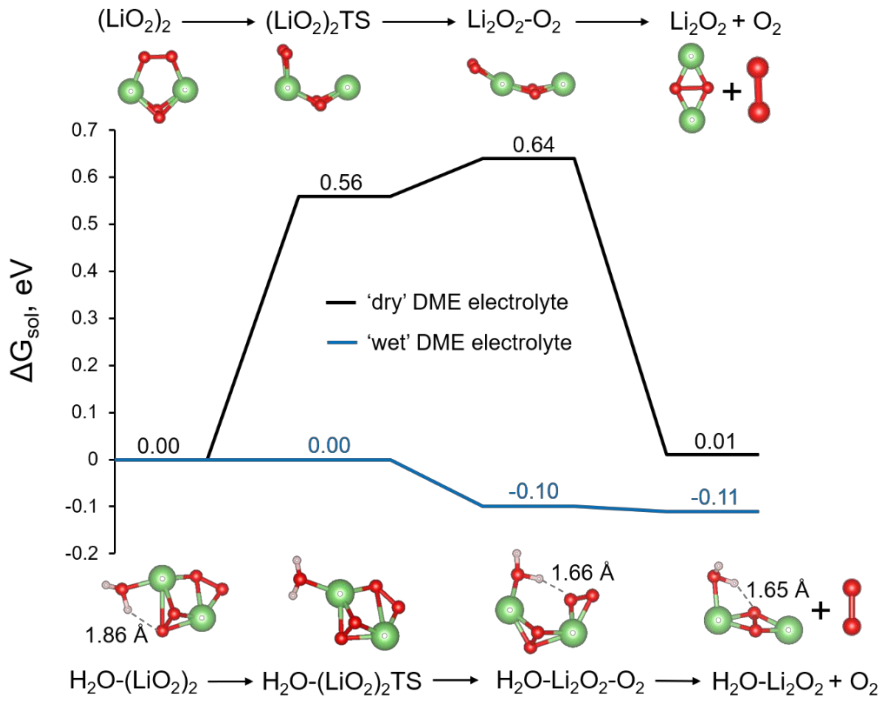

Figure 1 The reaction free energy (ΔG_{sol}) for disproportionation reaction in 'wet' (blue lines) and 'dry' (black lines) DME electrolytes based on G4MP2 calculations, referenced to H_2O-$(LiO_2)_2$ complex and LiO_2 dimer, respectively. The reaction free energies shown here include solvation corrections, corresponding to ΔG_{sol} of G4MP2 in Tables 1 and 2. Although the transition state was defined as the saddle point in the electronic energy between reactant and product, the free energy of the $(LiO_2)_2$ TS is lower than that of the Li_2O_2-O_2 complex in black lines because the B3LYP/6-31G(2df,p) geometry was used for G4MP2 calculation and the

solvation energy correction. The optimized ball-and-stick structures have Li, O and H in green, red and white, respectively.

We first discuss the 'wet' environment results in Figure 1, which refers to the DME electrolyte with a water molecule present. For this discussion the reaction energies (ΔE_o), reaction free energies in vacuum (ΔG) and with implicit solvation correction (ΔG_{sol}) from PBE(PW), B3LYP/6-31G(2df,p), B3LYP/6-311++G(2df,p) and G4MP2 calculations are summarized in Table 1. The reaction starts with a H_2O-$(LiO_2)_2$ complex, optimized at the B3LYP/6-31G(2df,p) level in which a Li-O bond formed between water and LiO_2 dimer, as shown in the left corner of the bottom panel of Figure 1. A hydrogen bond is present between O in the LiO_2 dimer and H in H_2O with a distance of 1.86 Å. A small barrier (ΔE_o for H_2O-$(LiO_2)_2$TS in Table 1) of 0.04 eV was obtained with the B3LYP/6-31G(2df,p) method. We note that for some initial geometries investigated, the disproportionation reaction with a water molecule is spontaneous and barrierless, but for the purposes of this study we have used the pathway with a slight barrier. The hydrogen bond between water and the LiO_2 dimer is gone in the transition state as illustrated in the H_2O-$(LiO_2)_2$TS geometry in Figure 1. A small barrier (ΔE_o for H_2O-$(LiO_2)_2$TS in Table 1), 0.05 eV, is also obtained at the G4MP2 level using the B3LYP/6-31G(2df,p) optimized geometry. With inclusion of solvation corrections, the G4MP2 relative free energy barrier (ΔG_{sol}) becomes negative (-0.08 eV) indicating no barrier and is plotted as 0 eV in Figure 1 (blue line). There is a very small barrier for PBE(PW) calculations as listed in Table 1. The reaction free energies for LiO_2 disproportionation from PBE(PW) calculations are plotted in Figure S1.

After crossing the small energy barrier, a H_2O-Li_2O_2-O_2 complex resulted with a hydrogen bond between water and the O_2 starting to leave in this complex (see Figure 1) with a distance of 1.66 Å. The ΔG_{sol} of the H_2O-Li_2O_2-O_2 complex is lower than that of the starting reactants by 0.11 eV at the B3LYP/6-31G(2df,p) level and by 0.10 eV at the G4MP2 level. Removal of the O_2 from the complex is significantly uphill (ΔE_o for H_2O-Li_2O_2 + O_2) by 0.86 eV at the B3LYP/6-31G(2df,p) level and by 0.66 eV at the G4MP2 level. However, the reaction free energy, ΔG_{sol}, becomes exothermic with a reaction free energy of -0.11 eV, as shown by the blue line in Figure 1. The resulting H_2O-Li_2O_2 complex has Li_2O_2 in a diamond shape (see the right corner configuration in

the bottom panel in Figure 1). The H_2O-Li_2O_2 complex also includes a hydrogen bond between water and Li_2O_2 with a distance of 1.65 Å.

In the 'wet' electrolyte, the reaction energies (ΔE_o) listed in Table 1, from the PBE(PW), B3LYP/6-31G(2df) and B3LYP/6-311++G(2df,p) calculations give the results in agreement with G4MP2 energies. The ΔG based on different levels of theories follows the same trend as (ΔE_o). With the implicit solvation effect included, all four theories indicate no barriers for disproportionation to a H_2O-Li_2O_2-O_2 complex. The ΔG_{sol} for H_2O-Li_2O_2 and O_2 formation obtained from PBE and G4MP2 are downhill (-0.08 and -0.11 eV), while the ones from B3LYP/6-31G(2df,p) calculations are slightly uphill (0.09 eV). The driving force for the small or no barrier found when a water molecule is involved in the disproportionation probably is because the water molecule interaction with one Li of the LiO_2 dimer (in H_2O-$(LiO_2)_2$) weakens the on-top O_2 (bound to both Li atoms) of the dimer, so the O_2 can rotate to bond with just one Li (in the H_2O-Li_2O_2-O_2 complex) as shown by the structures in Figure 1.

Table 1. The reaction energies (ΔE_o), reaction free energies in vacuum (ΔG) and in implicit DME solvent (ΔG_{sol}) at 298 K for the disproportionation reaction, $H_2O-(LiO_2)_2 \rightarrow H_2O-Li_2O_2 + O_2$, based on different levels of theory.

	Method	Relative Energy, eV			
		H_2O-$(LiO_2)_2$	H_2O-$(LiO_2)_2$TS[a]	H_2O-Li_2O_2-O_2 complex	H_2O-Li_2O_2 + O_2
ΔE_o	PBE(PW)	0.0	0.08	0.0	0.89
	B3LYP/6-31G(2df,p)	0.0	0.04[b]	-0.07	0.86
	B3LYP/6-311++G(2df,p)[c]	0.0	0.02	-0.08	0.70
	G4MP2[c]	0.0	0.05	-0.06	0.66
ΔG	PBE(PW)	0.0	0.02	-0.01	0.49
	B3LYP/6-31G(2df,p)	0.0	0.0	-0.05	0.49
	B3LYP/6-311++G(2df,p)[c]	0.0	-0.02	-0.05	0.33
	G4MP2[c]	0.0	-0.01	-0.04	0.29
ΔG_{sol}	PBE(PW)	0.0	0.00	-0.12	-0.08
	B3LYP/6-31G(2df,p)	0.0	-0.07	-0.11	0.09

B3LYP/6-311++G(2df,p)[c]	0.0	-0.08	-0.10	-0.01
G4MP2[c]	0.0	-0.08	-0.10	-0.11

[a]In some cases with inclusion of zero-point energy, entropy and solvation energies, the free energies of the TS become negative, although technically a barrier cannot be less than zero.

[b]Results given here is for a located transition state; in some cases depending on the starting geometry, the reaction is spontaneous to the H_2O-Li_2O_2-O_2 product. The structures at the located transition state is used for the G4MP2 and B3LYP/6-311++G(2df,p) single point energies.

[c]At B3LYP/6-31G(2df,p) geometry.

The G4MP2 energy profile for the disproportionation of the LiO_2 dimer in 'dry' environment is displayed with a black line in Figure 1 for comparison to that in the 'wet' environment. The geometries of reactant, transition state, disproportionation intermediate and final product are depicted in the top panel of Figure 1. The reaction energies (ΔE_o) and the free energies with/without solvation corrections ($\Delta G_{sol}/\Delta G$) for LiO_2 dimer disproportionation to Li_2O_2 and O_2 in 'dry' environment can be found in Table 2 at various levels of theory. Based on the B3LYP/6-31G(2df,p) optimization calculation, the LiO_2 dimer has a pentagonal shape in a triplet state (see the first inset configuration in the top panel of Figure 1). One of Li-O bonds breaks giving a disproportionation transition state with an energy barrier of 0.38 eV (ΔE_o for $(LiO_2)_2$TS in Table 2) according to B3LYP/6-31G(2df,p). With a single point energy calculation at G4MP2 level using the B3LYP/6-31G(2df,p) geometry, the energy barrier in a 'dry' DME electrolyte, ΔG, is 0.77 eV, which is much higher than that in 'wet' electrolyte, i.e. -0.01 eV in Table 1. With the solution correction at G4MP2 level, the energy barrier is decreased to 0.56 eV in 'dry' electrolyte.

The reaction free energy (ΔG_{sol}) for the Li_2O_2-O_2 complex formation without a water molecule present is computed as 0.14 eV at the B3LYP/6-31G(2df,p) level as shown in Table 2. The free energy in 'dry' DME (ΔG_{sol}) is 0.64 eV at G4MP2 level, which is even slightly higher than the energy of $(LiO_2)_2$TS as shown with black lines in Figure 1. This trend is because the G4MP2 calculations utilized the B3LYP/6-31G(2df,p) level geometry and the implicit solvation corrections. Removal of O_2 from the Li_2O_2-O_2 complex requires 0.70 eV energy (ΔE_o in Table 2) based on G4MP2 calculations. The free energy (ΔG in Table 2) for LiO_2 disproportionation to Li_2O_2 and O_2 is 0.36 eV at G4MP2 level, which is comparable with 0.29 eV based on

UCCSD(T)/CBS calculations of Bryantsev et al.[29] With solvation energy corrections, this reduces to 0.01 eV as shown in Figure 1.

As shown in Table 2, the PBE(PW), B3LYP/6-31G(2df,p) and B3LYP/6-311++G(2df,p) calculations resulted in the same trend of ΔE_o, ΔG and ΔG_{sol} for the LiO_2 disproportionation reaction as G4MP2. The energy barrier, ΔE_o, obtained from PBE(PW) is 0.28 eV, the lowest one among those from different theories. The low energy barrier from PBE(PW) is due to the 4-bridge structure of LiO_2 dimer (depicted in Figure S1) predicted by PBE(PW) compared to the twisted O_2 for B3LYP (see Figure 1). Based on G4MP2 energies of these two possible structures, the B3LYP result should be the correct configuration. The implicit solvation corrections exhibited different effects on the values of the energy barriers from different methods.

Table 2. The electronic reaction energies (ΔE_o), reaction free energies in vacuum (ΔG) and in implicit DME (ΔG_{sol}) at 298 K for $(LiO_2)_2 \rightarrow Li_2O_2 + O_2$, based on different level of theories.

	Method	Relative Energy, eV			
		$(LiO_2)_2$	$(LiO_2)_2$TS[a]	Li_2O_2-O_2 complex	Li_2O_2 + O_2
ΔE_o	PBE(PW)	0.0	0.28	0.18	1.12
	B3LYP/6-31G(2df,p)	0.0	0.38	0.35	0.97
	B3LYP/6-311++G(2df,p)[b]	0.0	0.37	0.36	0.83
	G4MP2[b]	0.0	0.75[c]	0.84	0.70
ΔG	PBE(PW)	0.0	0.11	0.03	0.66
	B3LYP/6-31G(2df,p)	0.0	0.38	0.28	0.63
	B3LYP/6-311++G(2df,p)[b]	0.0	0.37	0.29	0.49
	G4MP2[b]	0.0	0.77	0.77	0.36
ΔG_{sol}	PBE(PW)	0.0	-0.07	0.12	0.33
	B3LYP/6-31G(2df,p)	0.0	0.19	0.14	0.28
	B3LYP/6-311++G(2df,p)[b]	0.0	0.19	0.15	0.21
	G4MP2[b]	0.0	0.56[c]	0.64	0.01

[a]The G4MP2 and B3LYP values for the activation energy differ from those in Ref [30], which did not find the correct transition state.

[b]At B3LYP/6-31G(2df,p) geometry.

[c]The energy of $(LiO_2)_2$TS is higher than the energy of the Li_2O_2-O_2 complex due to the use of the G4MP2 single point calculation with the B3LYP/6-31G(2df,p) geometry and solvation correction.

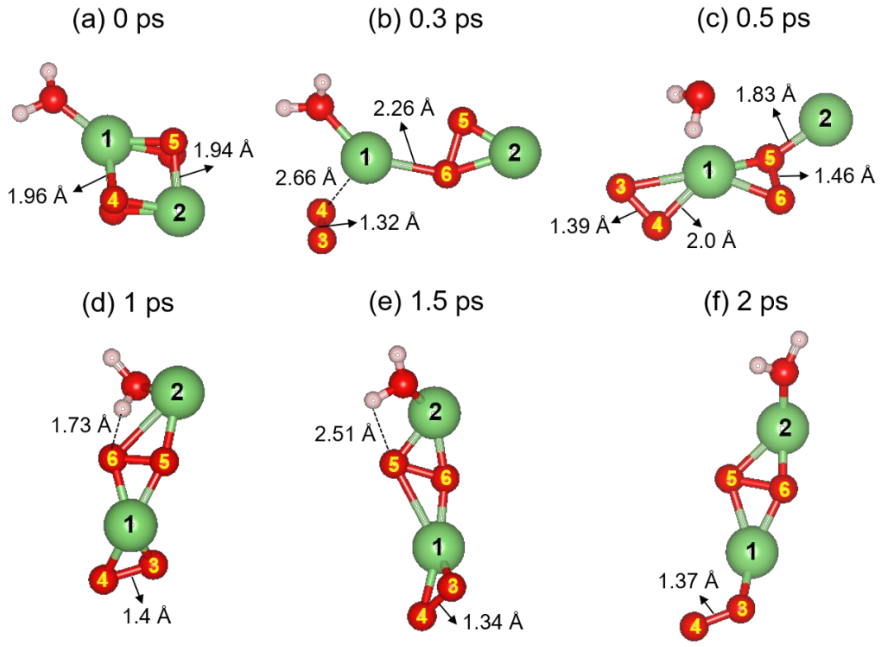

Figure 2. The structures at (a) 0 ps, (b) 0.3 ps, (c) 0.5 ps, (d) 1 ps, (e) 1.5 ps and (f) 2 ps for the disproportionation reaction in 'wet' DME electrolyte obtained from AIMD calculations at 300K. The O, H, and Li atoms are in red, white, and green, respectively. All the DME solvent molecules were hidden for the visualization purpose. The Li and O atoms are labeled with numbers one to six for visual guidance. The bond lengths of Li-O and O-O are in Å.

The LiO_2 disproportionation reaction in 'wet' DME electrolyte was also investigated using AIMD calculations with an explicit water molecule and DME molecules at constant temperature of 300 K. The PBE(PW) method was used for the AIMD calculations. The assumption that disproportionation occurs away from the surface in electrolyte is reasonable based on experimental evidence for discharge mechanisms.[45-48] The configuration of the simulation box for AIMD modeling can be found in Figure S2. Representative snapshots from AIMD calculations in 'wet' DME are displayed in Figure 2, the explicit DME molecules were removed for the visualization purpose. Two Li and four O atoms were labeled with numbers one to six for visual guidance. The initial structure was obtained from the optimized geometry at the ground state. We set a cutoff distance of H_2O-Li_2O_2 and O_2 (i.e. the bond length of No.1 Li and No.3/4 O) as 2.6 Å. As a result,

starting from the initial H_2O-$(LiO_2)_2$ complex, the disproportionation product H_2O-Li_2O_2 is formed around 0.3 ps (see Figure 2(b)). Because of the very shallow PBE(PW) energy landscape as listed in Table 1, the simulation snapshots indicate that O_2 and H_2O can leave and return to the complex during the simulation timescale, as demonstrated in Figure 2(b-f), suggesting the availability of these species for further discharge reactions. The AIMD calculations with explicit DME molecules provides the evidence that in the presence of one water molecule, the $(LiO_2)_2$ dimer will disproportionate to H_2O-Li_2O_2 plus O_2.

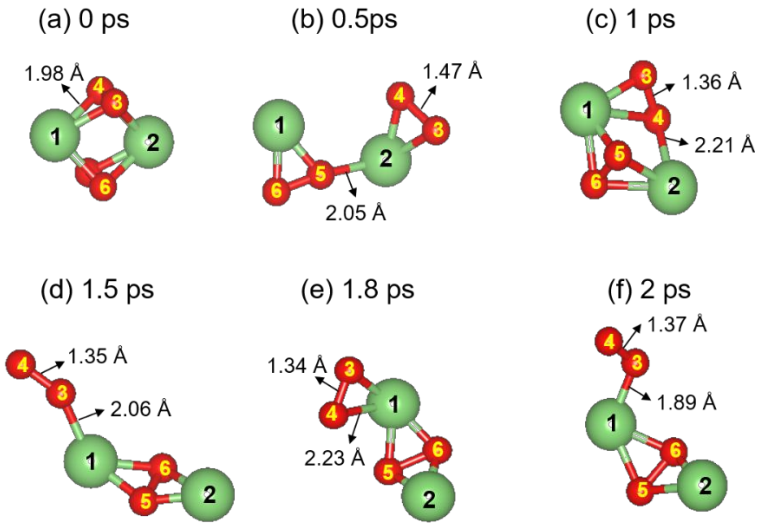

Figure 3. The structures at (a)0 ps, (b)0.5 ps, (c)1 ps, (d)1.5 ps, (e)1.8 ps and (f)2 ps for disproportionation reaction in 'dry' DME electrolyte obtained from AIMD calculations at 300K. The O and Li atoms are in red and green, respectively. All the DME solvent molecules were hidden for the visualization purpose. The Li and O atoms are labeled with No. 1-6 for visual guidance. The bond lengths of Li-O and O-O were labeled in Å.

Although the PBE(PW) method does not find a significant barrier for LiO_2 dimer disproportionation in 'dry' electrolyte (Table 2) as the other methods do, AIMD simulations using PBE(PW) for LiO_2 dimer disproportionation in 'dry' DME electrolyte at 300 K were also performed. Representative snapshots from AIMD calculations in 'dry' DME are displayed in Figure 3 with the explicit DME molecules hidden for the visualization purpose. Both Li and O atoms were labeled with numbers one to six for visual guidance. The starting structure was extracted from the geometry optimized at the ground state. In 'dry' DME electrolyte, during the

first one picosecond of the AIMD simulation, the LiO_2 dimer transformed its geometries as depicted in Figure 3(a-c). A disproportionation intermediate, Li_2O_2-O_2 complex, is formed around 1.5 ps (as shown in Figure 3(d)). Thus, these PBE(PW) results as expected indicate the disproportionation reaction occurs in 'dry' DME electrolyte as well and is consistent with the static PBE(PW) calculations, which give a no barrier (i.e. -0.07 eV in Table 2) for disproportionation. It is notable that in the 'dry' DME electrolyte, although we set a threshold of bond length for No.1 Li and No.3 O as 2.6 Å, we did not observe O_2 molecule leave and return during 2 ps as that in 'wet' electrolyte, which may indicate that the potential energy surface is not as shallow for the 'wet' electrolyte. We can see the Li_2O_2-O_2 complex present from 1.5 ps until 2 ps, as displayed in Figure 3(d-f) without the bond length of No.1 Li and No.3 O exceeding 2.6 Å.

Since the electrode surface could play some role in the reaction mechanism for Li_2O_2 formation during the discharge process, we investigated three possible reactions on an Au(100) surface with AIMD calculations using PBE(PW) method. The computational details of the results of these AIMD calculations can be found in ESI. The first two mechanisms were for LiO_2 disproportionation to Li_2O_2 in 'wet' and 'dry' DME electrolyte on the Au(100) surface and the results are in Figure S3-S4. The AIMD calculations indicate that the LiO_2 disproportionation reaction might proceed on Au(100) in both 'wet' and 'dry' DME electrolyte similar as for just in the electrolyte without the surface. We also calculated the LiO_2 adsorption on different Au surfaces. The favorable adsorption geometries and adsorption energies were demonstrated in Figure S5. The third mechanism was for a two-electron reaction for Li_2O_2 (as shown in Reaction (4)) where a H_2O molecule activates O_2 to catalyze the Li_2O_2 formation as proposed in Ref 18. The results are displayed in Figure S7 and it is indicates that water is not able to activate O_2 as proposed in Ref 18. We also note that these AIMD results including the surface also provide an explanation for the experimental observations that the dioxygen (O_2/O_2^-) electrochemistry is irreversible when Li^+ is added to the electrolyte (as shown in cyclic voltammetry curves in Figure 3a in Ref 18). The AIMD results show that the reduced oxygen (O_2^-) forms an ion pair with Li^+ (i.e. LiO_2), which is the reason the dioxygen electrochemistry becomes irreversible with addition of Li^+.

Our theoretical calculations for the disproportionation reaction in an implicit DME solvent provide an explanation for this enhanced Li_2O_2 formation observed experimentally in 'wet' DME electrolyte by Markovic et al.[18] The G4MP2 calculations indicate that it is more kinetically favorable when a water molecule is involved in the LiO_2 disproportionation to Li_2O_2 formation. This is consistent with the results of Markovic's work,[18] who compared the product distribution of the Li-O_2 discharge reactions in the electrolytes with 1 ppm of H_2O and 40 ppm of H_2O. According to their Raman spectra data, in the 1 ppm electrolyte only a LiO_2 peak was observed at ~1130 cm^{-1}, while in the 40 ppm electrolyte a strong Li_2O_2 peak at ~785 cm^{-1} appeared along with a LiO_2 peak with decreased intensity. These peaks were assigned based on previous experimental measurments[49], and they are consistent with our previous calculations[50] as well as some additional ones we carried out in this work (see Figure S8). We note that due to the relatively low barrier (i.e. 0.56 eV) and low reaction energy (i.e. 0.01 eV) in 'dry' electrolyte based on the G4MP2 method, disproportionation will eventually occur, which is why Li_2O_2 is generally the dominant product even without any water present in the experimental measurements, which occur over a relatively long time.

4. Conclusions

In summary, this study has utilized first-principles calculations to demonstrate that the very small amounts of water in the electrolyte is able to promote the LiO_2 disproportionation reaction to form Li_2O_2 in a Li-O_2 battery compared to when there is essentially no water present. The following conclusions can be drawn from the current work:

1. G4MP2 calculations show that the presence of a water molecule added to a LiO_2 dimer (i.e. in 'wet' electrolyte) makes disproportionation spontaneous, i.e., there is no barrier for the formation of Li_2O_2 plus an O_2 molecule. In contrast without a water molecule interacting with the LiO_2 dimer (i.e. in 'dry' electrolyte), there is a barrier of 0.56 eV associated with disproportionation reaction according to G4MP2, indicating that the LiO_2 dimer in such a case will be slower to disproportionate.
2. AIMD calculations in explicit DME electrolyte with the PBE(PW) functional provide additional evidence that in a 'wet' electrolyte, the H_2O-$(LiO_2)_2$ disproportionation to H_2O-Li_2O_2 plus O_2 will occur. Due to the very shallow PBE(PW) energy landscape similar to that

of G4MP2, the O_2 and H_2O are able to leave and return to the complex, indicating the availability of these species for further discharge reactions.

3. These theoretical calculations of the water effect on the LiO_2 disproportionation reaction provide an explanation for why Li_2O_2 formation is promoted in experiments using a DME electrolyte containing very small amounts of water ('wet' DME electrolyte) compared to that in 'dry' DME electrolyte.

Acknowledgement

The work by NS, PZ, NM and LAC was supported by the U.S. Department of Energy, BES-Materials Science and Engineering, under Contract DE-AC-02-06CH11357, with UChicago Argonne, LLC, the operator of Argonne National Laboratory. The work by ATN and PCR was supported by the U.S. Department of Energy, Office of Energy Efficiency and Renewable Energy, Vehicle Technologies Office. The authors are also thankful for the supercomputing time from Bebop cluster supported by Laboratory Computing Resource Center at Argonne National Laboratory (ANL) and Carbon cluster supported by Center for Nanoscale Materials (CNM) at ANL supported by the Office of Science of the US Department of Energy under the contract No. DE-AC02-06CH11357.

Author Contributions

NM, LAC, and PZ conceived the idea for the computational studies. NS carried out periodic calculations. PCR carried out cluster calculations. ATN performed AIMD calculations of Au surface. All authors contributed to the write up of the manuscript.

Conflict of Interest

The authors declare no conflict of interest.

1. Lu, J.; Li, L.; Park, J.-B.; Sun, Y.-K.; Wu, F.; Amine, K., Aprotic and Aqueous Li–O_2 Batteries. *Chemical Reviews* **2014,** *114* (11), 5611-5640.

2. Bruce, P. G.; Freunberger, S. A.; Hardwick, L. J.; Tarascon, J.-M., Li–O_2 and Li–S batteries with high energy storage. *Nature Materials* **2012,** *11* (1), 19-29.

3. Peng, Z.; Freunberger, S. A.; Chen, Y.; Bruce, P. G., A Reversible and Higher-Rate Li-O_2 Battery. *Science* **2012,** *337* (6094), 563.

4. Girishkumar, G.; McCloskey, B.; Luntz, A. C.; Swanson, S.; Wilcke, W., Lithium−Air Battery: Promise and Challenges. *Journal of Physical Chemistry Letters* **2010,** *1* (14), 2193-2203.
5. Lu, Y.-C.; Gallant, B. M.; Kwabi, D. G.; Harding, J. R.; Mitchell, R. R.; Whittingham, M. S.; Shao-Horn, Y., Lithium–oxygen batteries: bridging mechanistic understanding and battery performance. *Energy & Environmental Science* **2013,** *6* (3), 750-768.
6. Freunberger, S. A.; Chen, Y.; Peng, Z.; Griffin, J. M.; Hardwick, L. J.; Bardé, F.; Novák, P.; Bruce, P. G., Reactions in the Rechargeable Lithium–O_2 Battery with Alkyl Carbonate Electrolytes. *Journal of the American Chemical Society* **2011,** *133* (20), 8040-8047.
7. Lim, H.-D.; Lee, B.; Bae, Y.; Park, H.; Ko, Y.; Kim, H.; Kim, J.; Kang, K., Reaction chemistry in rechargeable Li–O2 batteries. *Chemical Society Reviews* **2017,** *46* (10), 2873-2888.
8. Wang, Y.; Lu, Y.-C., Nonaqueous Lithium–Oxygen batteries: Reaction mechanism and critical open questions. *Energy Storage Materials* **2020,** *28*, 235-246.
9. Lai, J.; Xing, Y.; Chen, N.; Li, L.; Wu, F.; Chen, R., Electrolytes for Rechargeable Lithium–Air Batteries. *Angewandte Chemie International Edition* **2020,** *59* (8), 2974-2997.
10. Ye, L.; Liao, M.; Sun, H.; Yang, Y.; Tang, C.; Zhao, Y.; Wang, L.; Xu, Y.; Zhang, L.; Wang, B.; Xu, F.; Sun, X.; Zhang, Y.; Dai, H.; Bruce, P. G.; Peng, H., Stabilizing Lithium into Cross-Stacked Nanotube Sheets with an Ultra-High Specific Capacity for Lithium Oxygen Batteries. *Angewandte Chemie International Edition* **2019,** *58* (8), 2437-2442.
11. Asadi, M.; Sayahpour, B.; Abbasi, P.; Ngo, A. T.; Karis, K.; Jokisaari, J. R.; Liu, C.; Narayanan, B.; Gerard, M.; Yasaei, P.; Hu, X.; Mukherjee, A.; Lau, K. C.; Assary, R. S.; Khalili-Araghi, F.; Klie, R. F.; Curtiss, L. A.; Salehi-Khojin, A., A lithium–oxygen battery with a long cycle life in an air-like atmosphere. *Nature* **2018,** *555* (7697), 502-506.
12. Park, J.-B.; Lee, S. H.; Jung, H.-G.; Aurbach, D.; Sun, Y.-K., Redox Mediators for Li–O_2 Batteries: Status and Perspectives. *Advanced Materials* **2018,** *30* (1), 1704162.
13. Kwak, W.-J.; Lau, K. C.; Shin, C.-D.; Amine, K.; Curtiss, L. A.; Sun, Y.-K., A Mo_2C/Carbon Nanotube Composite Cathode for Lithium–Oxygen Batteries with High Energy Efficiency and Long Cycle Life. *ACS Nano* **2015,** *9* (4), 4129-4137.
14. Dai, A.; Li, Q.; Liu, T.; Amine, K.; Lu, J., Fundamental Understanding of Water-Induced Mechanisms in Li–O2 Batteries: Recent Developments and Perspectives. *Advanced Materials* **2019,** *31* (31), 1805602.
15. Aetukuri, N. B.; McCloskey, B. D.; García, J. M.; Krupp, L. E.; Viswanathan, V.; Luntz, A. C., Solvating additives drive solution-mediated electrochemistry and enhance toroid growth in non-aqueous Li–O_2 batteries. *Nature Chemistry* **2015,** *7* (1), 50-56.
16. Schwenke, K. U.; Metzger, M.; Restle, T.; Piana, M.; Gasteiger, H. A., The Influence of Water and Protons on Li_2O_2 Crystal Growth in Aprotic Li-O_2 Cells. *Journal of The Electrochemical Society* **2015,** *162* (4), A573-A584.
17. Kwabi, D. G.; Batcho, T. P.; Feng, S.; Giordano, L.; Thompson, C. V.; Shao-Horn, Y., The effect of water on discharge product growth and chemistry in Li–O2 batteries. *Physical Chemistry Chemical Physics* **2016,** *18* (36), 24944-24953.
18. Staszak-Jirkovský, J.; Subbaraman, R.; Strmcnik, D.; Harrison, K. L.; Diesendruck, C. E.; Assary, R.; Frank, O.; Kobr, L.; Wiberg, G. K. H.; Genorio, B.; Connell, J. G.; Lopes, P. P.; Stamenkovic, V. R.; Curtiss, L.; Moore, J. S.; Zavadil, K. R.; Markovic, N. M., Water as a Promoter and Catalyst for Dioxygen Electrochemistry in Aqueous and Organic Media. *ACS Catalysis* **2015,** *5* (11), 6600-6607.
19. Johnson, L.; Li, C.; Liu, Z.; Chen, Y.; Freunberger, S. A.; Ashok, P. C.; Praveen, B. B.; Dholakia, K.; Tarascon, J.-M.; Bruce, P. G., The role of LiO_2 solubility in O_2 reduction in aprotic solvents and its consequences for Li–O_2 batteries. *Nature Chemistry* **2014,** *6* (12), 1091-1099.

20. Ma, S.; Wang, J.; Huang, J.; Zhou, Z.; Peng, Z., Unveiling the Complex Effects of H_2O on Discharge–Recharge Behaviors of Aprotic Lithium–O_2 Batteries. *Journal of Physical Chemistry Letters* **2018,** *9* (12), 3333-3339.
21. Qiao, Y.; Wu, S.; Yi, J.; Sun, Y.; Guo, S.; Yang, S.; He, P.; Zhou, H., From O_2^- to HO_2^-: Reducing By-Products and Overpotential in Li-O_2 Batteries by Water Addition. *Angewandte Chemie International Edition* **2017,** *56* (18), 4960-4964.
22. Liu, T.; Leskes, M.; Yu, W.; Moore, A. J.; Zhou, L.; Bayley, P. M.; Kim, G.; Grey, C. P., Cycling Li-O_2 batteries via LiOH formation and decomposition. *Science* **2015,** *350* (6260), 530.
23. Li, F.; Wu, S.; Li, D.; Zhang, T.; He, P.; Yamada, A.; Zhou, H., The water catalysis at oxygen cathodes of lithium–oxygen cells. *Nature Communications* **2015,** *6* (1), 7843.
24. Torres, A. E.; Balbuena, P. B., Exploring the LiOH Formation Reaction Mechanism in Lithium–Air Batteries. *Chemistry of Materials* **2018,** *30* (3), 708-717.
25. Zhu, Y. G.; Liu, Q.; Rong, Y.; Chen, H.; Yang, J.; Jia, C.; Yu, L.-J.; Karton, A.; Ren, Y.; Xu, X.; Adams, S.; Wang, Q., Proton enhanced dynamic battery chemistry for aprotic lithium–oxygen batteries. *Nature Communications* **2017,** *8* (1), 14308.
26. Liu, T.; Kim, G.; Jónsson, E.; Castillo-Martinez, E.; Temprano, I.; Shao, Y.; Carretero-González, J.; Kerber, R. N.; Grey, C. P., Understanding LiOH Formation in a Li-O_2 Battery with LiI and H_2O Additives. *ACS Catalysis* **2019,** *9* (1), 66-77.
27. Wang, M.; Yao, Y.; Bi, X.; Zhao, T.; Zhang, G.; Wu, F.; Amine, K.; Lu, J., Optimization of oxygen electrode combined with soluble catalyst to enhance the performance of lithium–oxygen battery. *Energy Storage Materials* **2020,** *28*, 73-81.
28. Laoire, C. O.; Mukerjee, S.; Abraham, K. M.; Plichta, E. J.; Hendrickson, M. A., Elucidating the Mechanism of Oxygen Reduction for Lithium-Air Battery Applications. *Journal of Physical Chemistry C* **2009,** *113* (46), 20127-20134.
29. Bryantsev, V. S.; Blanco, M.; Faglioni, F., Stability of Lithium Superoxide LiO_2 in the Gas Phase: Computational Study of Dimerization and Disproportionation Reactions. *Journal of Physical Chemistry A* **2010,** *114* (31), 8165-8169.
30. Das, U.; Lau, K. C.; Redfern, P. C.; Curtiss, L. A., Structure and Stability of Lithium Superoxide Clusters and Relevance to Li–O_2 Batteries. *Journal of Physical Chemistry Letters* **2014,** *5* (5), 813-819.
31. Becke, A. D., Density‐functional thermochemistry. III. The role of exact exchange. *Journal of Chemical Physics* **1993,** *98* (7), 5648-5652.
32. Lee, C.; Yang, W.; Parr, R. G., Development of the Colle-Salvetti correlation-energy formula into a functional of the electron density. *Physical Review B* **1988,** *37* (2), 785-789.
33. Perdew, J. P.; Burke, K.; Ernzerhof, M., Generalized Gradient Approximation Made Simple. *Physical Review Letters* **1996,** *77* (18), 3865-3868.
34. Frisch, M. J.; Trucks, G. W.; Schlegel, H. B.; Scuseria, G. E.; Robb, M. A.; Cheeseman, J. R.; Scalmani, G.; Barone, V.; Mennucci, B.; Petersson, G. A.; al, e., Gaussian 09 Revision E.01. *Gaussian, Inc., Wallingford CT* **2009**.
35. Kresse, G.; Furthmüller, J., Efficient iterative schemes for ab initio total-energy calculations using a plane-wave basis set. *Physical Review B* **1996,** *54* (16), 11169-11186.
36. Curtiss, L. A.; Redfern, P. C.; Raghavachari, K., Gaussian-4 theory using reduced order perturbation theory. *Journal of Chemical Physics* **2007,** *127* (12), 124105.
37. Curtiss, L. A.; Redfern, P. C.; Raghavachari, K., Assessment of Gaussian-4 theory for energy barriers. *Chemical Physics Letters* **2010,** *499* (1), 168-172.
38. Curtiss, L. A.; Redfern, P. C.; Raghavachari, K., Gaussian-4 theory. *The Journal of Chemical Physics* **2007,** *126* (8), 084108.

39. Cancès, E.; Mennucci, B.; Tomasi, J., A new integral equation formalism for the polarizable continuum model: Theoretical background and applications to isotropic and anisotropic dielectrics. *Journal of Chemical Physics* **1997,** *107* (8), 3032-3041.
40. Tomasi, J.; Mennucci, B.; Cammi, R., Quantum Mechanical Continuum Solvation Models. *Chemical Reviews* **2005,** *105* (8), 2999-3094.
41. Cheng, L.; Redfern, P.; Lau, K. C.; Assary, R. S.; Narayanan, B.; Curtiss, L. A., Computational Studies of Solubilities of LiO_2 and Li_2O_2 in Aprotic Solvents. *Journal of The Electrochemical Society* **2017,** *164* (11), E3696-E3701.
42. Sinha, P.; Boesch, S. E.; Gu, C.; Wheeler, R. A.; Wilson, A. K., Harmonic Vibrational Frequencies: Scaling Factors for HF, B3LYP, and MP2 Methods in Combination with Correlation Consistent Basis Sets. *Journal of Physical Chemistry A* **2004,** *108* (42), 9213-9217.
43. Blöchl, P. E., Projector augmented-wave method. *Physical Review B* **1994,** *50* (24), 17953-17979.
44. Nosé, S., A molecular dynamics method for simulations in the canonical ensemble. *Molecular Physics* **1984,** *52* (2), 255-268.
45. Lu, J.; Cheng, L.; Lau, K. C.; Tyo, E.; Luo, X.; Wen, J.; Miller, D.; Assary, R. S.; Wang, H.-H.; Redfern, P.; Wu, H.; Park, J.-B.; Sun, Y.-K.; Vajda, S.; Amine, K.; Curtiss, L. A., Effect of the size-selective silver clusters on lithium peroxide morphology in lithium–oxygen batteries. *Nature Communications* **2014,** *5* (1), 4895.
46. Aurbach, D.; McCloskey, B. D.; Nazar, L. F.; Bruce, P. G., Advances in understanding mechanisms underpinning lithium–air batteries. *Nature Energy* **2016,** *1* (9), 16128.
47. Zhang, Y.; Zhang, X.; Wang, J.; McKee, W. C.; Xu, Y.; Peng, Z., Potential-Dependent Generation of O_2^- and LiO_2 and Their Critical Roles in O_2 Reduction to Li_2O_2 in Aprotic Li–O_2 Batteries. *Journal of Physical Chemistry C* **2016,** *120* (7), 3690-3698.
48. Mahne, N.; Fontaine, O.; Thotiyl, M. O.; Wilkening, M.; Freunberger, S. A., Mechanism and performance of lithium–oxygen batteries – a perspective. *Chemical Science* **2017,** *8* (10), 6716-6729.
49. Peng, Z.; Freunberger, S. A.; Hardwick, L. J.; Chen, Y.; Giordani, V.; Bardé, F.; Novák, P.; Graham, D.; Tarascon, J.-M.; Bruce, P. G., Oxygen Reactions in a Non-Aqueous Li^+ Electrolyte. *Angewandte Chemie International Edition* **2011,** *50* (28), 6351-6355.
50. Yang, J.; Zhai, D.; Wang, H.-H.; Lau, K. C.; Schlueter, J. A.; Du, P.; Myers, D. J.; Sun, Y.-K.; Curtiss, L. A.; Amine, K., Evidence for lithium superoxide-like species in the discharge product of a Li–O2 battery. *Physical Chemistry Chemical Physics* **2013,** *15* (11), 3764-3771.